JOURNAL OF THERMOPHYSICS AND HEAT TRANSFER
Vol. 11, No. 4, October–December 1997

State-to-State Approach in the Kinetics of Air Components Under Re-Entry Conditions

M. Capitelli,* I. Armenise,† and C. Gorse*
University of Bari, Bari 70126, Italy

A state-to-state vibrational kinetics for air components including recombination–dissociation processes as well as the formation of NO through the reaction between vibrationally excited nitrogen molecules and atomic oxygen has been inserted in a monodimensional fluid dynamic code, describing the boundary layer surrounding a body under re-entry conditions. The results show that the formation of NO is strongly enhanced by the nonequilibrium vibrational distribution of N_2 formed during the recombination process. This kind of distribution is responsible for the non-Arrhenius behavior of dissociation constants of N_2 and O_2 as well as the NO formation rate as a function of instantaneous temperature.

Nomenclature

B = kinetic terms
c_p = specific heat at constant pressure including only rotational and translational degrees of freedom
c_v = $\rho_v(\eta)/\rho(\eta)$
E_v = vibrational energy of the vth vibrational level
$f(\eta)$ = stream function
k_d = pseudo-first-order dissociation constant
k_f = pseudo-first-order formation rate
p_e = pressure
T_e = temperature at the edge of the boundary layer
T_w = wall temperature
u_e = longitudinal speed at the edge of the boundary layer
$V–T$ = vibrational–translational energy exchange processes
$V–V$ = vibrational–vibrational energy exchange processes
x = body-parallel coordinate
y = body-normal coordinate
β = du_e/dx
η = body-normal coordinate
ϑ = $T(\eta)/T_e$
ξ = body-parallel coordinate
$\rho_v(\eta)$ = local mass density of molecules in the vth vibrational state
$\rho(\eta)$ = local total mass density

Introduction

NONEQUILIBRIUM vibrational distributions and non-Arrhenius behavior of dissociation constants of nitrogen in the boundary layer of hypersonic flows have been recently discussed by our group. This behavior was attributed to the pumping of high N_2 vibrational levels through the recombination process, followed by the redistribution of the introduced vibrational quanta by $V–V$ and $V–T$ energy transfer processes. These results were obtained by using a state-to-state vibrational kinetics, the so-called ladder climbing model, coupled to the fluid dynamics of the boundary layer.[1–3] The resulting model consists of a system of second-order differential equations describing each vibrational level of the molecular manifold, plus an equation for the atoms and an equation for the gas temperature.[4–6]

In this paper we have extended this model to air; i.e., to a mixture of N_2 and O_2. The new model solves, always in the boundary-layer approximation, the vibrational kinetics of N_2, one for O_2 and an equation for the concentration of NO. In particular, the formation of NO is mainly described by the following process:

$$N_2(v) + O \rightarrow NO + N$$

the rate of which is strongly affected by the nonequilibrium vibrational distribution of N_2.

The results are then analyzed as a function of the different parameters entering the theory; i.e., p_e in the boundary layer, T_w, the temperature at the edge of the boundary layer T_e, and the inverse of the residence time in the boundary layer β. The variation of these parameters, especially near the surface that is considered noncatalytic, changes the importance of the different elementary energy exchange processes inserted in the vibrational kinetics. As an example, strong temperatures at the edge of the boundary layer (T_e = 7000 K), accompanied by high surface temperatures (T_w = 1000 K) emphasize the role of the recombination process in affecting the vibrational distribution of N_2; whereas lower T_e and T_w temperatures exalt the role of the $V–V$ up-pumping mechanism to the same goal.[3]

Another interesting aspect in this paper is the dependence of the concentration profiles on the rate coefficients used in the model. In particular, the dependence of the NO profile in the boundary layer on the adopted set of state-to-state rates of the preceding equation is discussed. Finally, the similarity between the present results and those occurring in expansion flows will be discussed.

Kinetic Problem

The vibrational kinetics of air mixtures includes the following processes:

$$N_2(v) + N_2(w) \leftrightarrow N_2(v-1) + N_2(w+1) \quad (1)$$

$$N_2(v) + N_2 \leftrightarrow N_2(v-1) + N_2 \quad (2)$$

$$N_2(v) + N \leftrightarrow N_2(w) + N \quad (3)$$

Received June 14, 1996; presented as Paper 96-1985 at the AIAA 27th Fluid Dynamics Conference, New Orleans, LA, June 17–20, 1996; revision received March 20, 1997; accepted for publication May 27, 1997.

*Professor, Chemistry Department, Centro di Studio per la Chimica dei Plasmi del CNR, Via Orabona 4.

†Researcher, Chemistry Department, Centro di Studio per la Chimica dei Plasmi del CNR, Via Orabona 4.

$$O_2(v) + O_2(w) \leftrightarrow O_2(v-1) + O_2(w+1) \quad (4)$$

$$O_2(v) + O_2 \leftrightarrow O_2(v-1) + O_2 \quad (5)$$

$$O_2(v) + O \leftrightarrow O_2(v-1) + O \quad (6)$$

$$O_2(v) + N_2 \leftrightarrow O_2(v-1) + N_2 \quad (7)$$

$$N_2(v) + O \leftrightarrow N_2(v-1) + O \quad (8)$$

$$N_2(v) + O \leftrightarrow NO + N \quad (9)$$

$$N + O_2 \leftrightarrow NO + O \quad (10)$$

$$NO + M \leftrightarrow N + O + M \quad (11)$$

Basically, we solve a vibrational kinetics for N_2 and O_2 coupled together through reactions (7–11). Reactions (9–11) are the main channels forming and destroying NO.

Concerning the dissociation–recombination reactions for N_2 and O_2, we consider a pseudolevel $(v' + 1)$ located just above the last bound level of the diatom (v'), through which passes the dissociation-recombination reaction; i.e., we consider the following elementary processes[4]:

$$N_2(v) + N_2(v') \leftrightarrow N_2(v-1) + N_2(v'+1) \leftrightarrow N_2(v-1) + 2N \quad (12)$$

$$N_2(v') + N_2 \leftrightarrow N_2(v'+1) + N_2 \leftrightarrow 2N + N_2 \quad (13)$$

$$N_2(v) + N \leftrightarrow N_2(v'+1) + N \leftrightarrow 3N \quad (14)$$

$$O_2(v) + O_2(v') \leftrightarrow O_2(v-1) + O_2(v'+1) \leftrightarrow O_2(v-1) + 2O \quad (15)$$

$$O_2(v') + O_2 \leftrightarrow O_2(v'+1) + O_2 \leftrightarrow 2O + O_2 \quad (16)$$

$$O_2(v') + O \leftrightarrow O_2(v'+1) + O \leftrightarrow 3O \quad (17)$$

In the zero-dimensional kinetics, we write a set of coupled first-order differential equations, giving the temporal evolution of each vibrational level in the presence of the elementary processes reported in the preceding text. In this approach, the density of the atomic species is seen as two times the concentration of the corresponding pseudolevel. For NO we consider only the ground vibrational level.

Input Data

In previous works[5–9] we have reported the rate coefficients of V–V and V–T processes involving vibrationally excited nitrogen molecules with nitrogen molecules and atomic nitrogen, and so we will report here the rate coefficients of the other processes.

The rates of processes (4–6), involving oxygen molecules and atoms, can be denoted as $KO^{w,w+1}_{v+1,v}$, $K2O_{v,v-1}$, and $K1O_{v,v-1}$, respectively. They have been put in the following analytical form by interpolating and extrapolating the values given in Refs. 10 and 11:

$$KO^{w,w+1}_{v+1,v} = 2.8 \times 10^{-18} T^{3/2} (v+1)(w+1) \times \exp[2.4(v-w)/\sqrt{T}] \quad \text{cm}^3/(\text{s} \times \text{part}) \quad (18)$$

with $v \leq w$:

$$K2O_{v,v-1} = v \times a \times \exp[b \times (v-1)] \quad \text{cm}^3/(\text{s} \times \text{part}) \quad (19)$$

with $a = T/[1.8 \times 10^{-20} \exp(122/T^{1/3}) \times [1 - \exp(-2273.7/T)]$ and $b = 2.99/\sqrt{T}$:

$$K1O_{v,v-1} = (3v-2) \frac{E^O_1 - E^O_0}{12.4 \times 10^{-2}} \times \frac{0.7 \times 10^{-13}}{\exp(30/T^{1/3})} \quad \text{cm}^3/(\text{s} \times \text{part}) \quad (20)$$

in which oxygen vibrational energy E^O is in cm^{-1}.

The rates of the V–T processes (7) and (8), involving both nitrogen and oxygen are, respectively, $P2O_{v,v-1}$ and $P1N_{v,v-1}$; for these rates we have used the following closed forms based on the data of Refs. 12 and 13:

$$P2O_{1,0} = 1/[3.8 \times 10^{-21} \times T \times \exp(140/T^{1/3}) \times [1 - \exp(-3394,9/T)]]$$

$$P2O_{v,v-1} = v \times \text{P2O}_{1,0} \times \exp[4.5(v-1)/\sqrt{T}] \quad \text{cm}^3/(\text{s} \times \text{part}) \quad (21)$$

$$P1N_{v,v-1} = 5 \times 10^{-12} \times v \times \exp[1.58(v-1)/\sqrt{T}] \times \exp(-128/\sqrt{T}) \quad \text{cm}^3/(\text{s} \times \text{part}) \quad (22)$$

The reaction rates involving $N_2(v)$ and atomic oxygen [process (9)] have been calculated according to the following expressions[14]:

$$Q^{O,NO}_{N_2(v),N} = e^{a1} \times \frac{(E_v + 3000)^{a2}}{T^{a3}} \times \exp[38370 \times a4/T + E_v \times a5/T)] \quad \text{cm}^3/(\text{s} \times \text{part}) \quad (23)$$

with $E_v = 3395 \times v \times [1 - 6.217 \times 10^{-2} \times (v+1)]$

The parameters $a1$, $a2$, $a3$, $a4$, and $a5$ entering the equation take different values, depending on the vibrational quantum level range. For $v = 0$–8 these parameters assume the following values: $a1 = -23.044680$, $a2 = -0.419312$, $a3 = -0.37836$, $a4 = 0.99243$, and $a5 = 0.989385$. For $v = 9$–12 they read: $a1 = 1.423118$, $a2 = -3.42306$, $a3 = -1.4234$, $a4 = -0.919692$, and $a5 = 0.917323$. Finally, for $v = 13$–23 we have: $a1 = -96.75885$, $a2 = 6.480504$, $a3 = -0.279371$, $a4 = -0.037869$, and $a5 = 0.019647$. The last parameters have also been used to extend the v range up to the last considered vibrational level of nitrogen, i.e., $v = 45$. The coefficients of process (10) are given[15]:

$$Q^{NO,N}_{O,O_2} = \frac{8.4 \times 10^{12} \times \exp(-19450/T)}{6.023 \times 10^{23}} \quad \text{cm}^3/(\text{s} \times \text{part}) \quad (24)$$

Finally, the rates of NO dissociation process (11) are the following[14]:

$$Q^{N_2} = 5 \times 10^{15} \times \exp(-75500/T)/(6.023 \times 10^{23}) \quad \text{cm}^3/(\text{s} \times \text{part}) \quad (25)$$

$$Q^{N} = 1.1 \times 10^{17} \times \exp(-75500/T)/(6.023 \times 10^{23}) \quad \text{cm}^3/(\text{s} \times \text{part}) \quad (26)$$

$$Q^{O_2} = 5 \times 10^{15} \times \exp(-75500/T)/(6.023 \times 10^{23}) \quad \text{cm}^3/(\text{s} \times \text{part}) \quad (27)$$

$$Q^{O} = 1.1 \times 10^{17} \times \exp(-75500/T)/(6.023 \times 10^{23}) \quad \text{cm}^3/(\text{s} \times \text{part}) \quad (28)$$

$$Q^{NO} = 1.1 \times 10^{17} \times \exp(-75500/T)/(6.023 \times 10^{23}) \quad \text{cm}^3/(\text{s} \times \text{part}) \quad (29)$$

The rates of the reverse processes have been obtained by using the detailed balance principle. This method has been also applied to obtain the rates from the pseudolevel to the other levels, whereas the excitation rates to the pseudolevel have been obtained by extrapolating the bound–bound transitions to bound–continuum ones. This point is the weaker point of the ladder-climbing model.[3]

Reaction (9) plays an important role in our results: use of Eq. (23) yields some discontinuity in the vibrational distribution of N_2. The following alternative equations[16] have been proposed is:

$$Q^{\mathrm{O,NO}}_{\mathrm{N_2}(v),\mathrm{N}} = 1.3 \times 10^{-10} \times \exp(-38000/T) \quad \text{if} \quad v = 0\text{–}12 \tag{30}$$

$$Q^{\mathrm{O,NO}}_{\mathrm{N_2}(v),\mathrm{N}} = 10^{-11} \quad \text{if} \quad v = 13\text{–}45 \tag{31}$$

for the direct processes and

$$Q^{\mathrm{NO,O}}_{\mathrm{N,N_2}(v)} = \frac{1.8 \times 10^{-11}}{2} \times \frac{T}{300} \quad \text{if} \quad v = 3, 4 \tag{32}$$

$$Q^{\mathrm{NO,O}}_{\mathrm{N,N_2}(v)} = 0 \quad \text{if} \quad v \neq 3, 4 \tag{33}$$

for the reverse ones. We have used both formulations to assess the dependence of our results to process (9).

Boundary-Layer Equations

The kinetic model has been inserted in the fluid dynamic equations describing the boundary layer surrounding the body flying at hypersonic velocity.

The resulting system of differential equations assume the following form:

$$C_v'' + f \times Sc \times C_v' = -\sum_{i=0}^{81} B(v, i) \times C_i \quad v = 0\text{–}81 \tag{34}$$

$$\begin{aligned}\vartheta'' + f \times Pr \times \vartheta' = {} & \sum_{v=0}^{46} \frac{Le}{c_p \times T_e} \times E_v^{\mathrm{N_2}} \left[\sum_{i=0}^{81} B(v, i) C_i\right] \\ & + \sum_{v=47}^{80} \frac{Le}{c_p \times T_e} \times E_v^{\mathrm{O_2}} \left[\sum_{i=0}^{81} B(v, i) C_i\right] \\ & + \sum_{v=81}^{81} \frac{Le}{c_p \times T_e} \times E_v^{\mathrm{NO}} \left[\sum_{i=0}^{81} B(v, i) C_i\right]\end{aligned} \tag{35}$$

The first 82 equations are the continuity equations of each species: 45 vibrational levels of nitrogen molecules, one pseudolevel representing nitrogen atoms, 33 vibrational levels of oxygen molecules, a pseudolevel for oxygen atoms, and one equation for NO molecules considered only in the ground state. The last equation is the energy one. Electronically excited states as well as free electrons were completely ignored.

In these equations, $C_v = \rho_v/\rho$, ρ_v is the mass density of the vth vibrational level, ρ is the total mass density, and $\vartheta = T/T_e$ is the ratio between the gas temperature in the boundary layer and the temperature at the edge of the boundary layer.

The derivatives have been performed with respect to the coordinate normal to the surface η, that is the only direction considered in our calculations thanks to the Lees–Dorodnitsyn coordinate transformations:

$$\xi = \int_0^x \rho_e u_e \, \mathrm{d}x \tag{36}$$

$$\eta = \frac{u_e}{\sqrt{2\xi}} \int_0^y \rho \, \mathrm{d}y \tag{37}$$

Therefore, we have calculated nitrogen and oxygen vibrational distribution functions, atomic nitrogen, atomic oxygen and NO population densities, and temperature along the coordinate η normal to the surface.

The following boundary conditions have been considered at the edge of the boundary layer ($\eta = 4$): fixed values of temperature ($T = T_e$), density ($\rho = \rho_e$), and pressure ($p = p_e$), together with equilibrium vibrational distribution functions $c_v = (c_v)_e$, while on the surface a fixed temperature $T = T_w$ and noncatalytic wall $(\partial c_v/\partial y)_w = 0$. Moreover, at $\eta = 4$, the concentrations of N_2, N, O_2, O, and NO are approximately those corresponding to equilibrium at T_e and p_e (Ref. 3).

The parameters entering the theory are the pressure, the temperatures T_e and T_w, and the β value, which in this approach

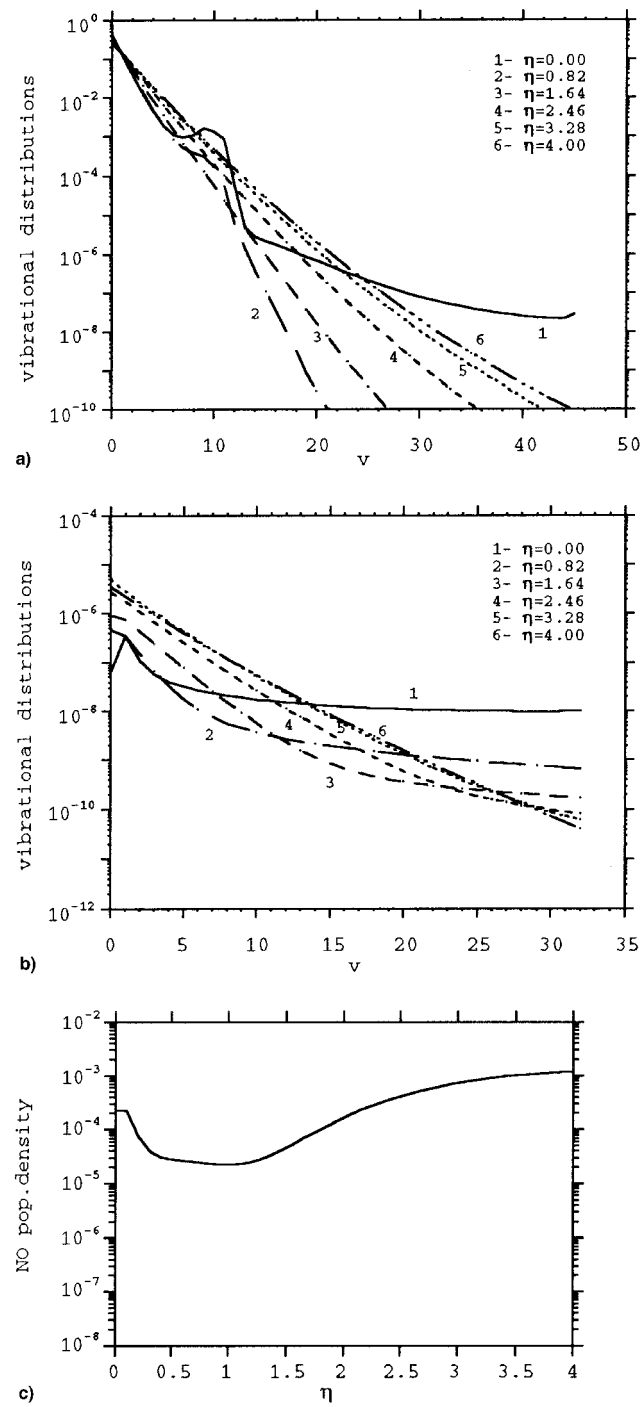

Fig. 1 Vibrational distributions of a) N_2 and b) O_2 at different η values, and c) NO profile as a function of η at $T_w = 300$ K, $T_e = 5000$ K, $p_e = 1000$ N/m^2, and $\beta = 5000$ s^{-1}.

can be considered as the inverse of the residence time of the particles in the boundary layer. The corresponding values have been selected for reproducing realistic flow conditions.[6]

Details about the boundary-layer equations as well as the ladder climbing model used for the kinetics can be found in Refs. 1–6, 17, and 18.

Results

Vibrational Distributions and NO Profiles

Let us first discuss the form of the vibrational distributions of N_2 and O_2 in the boundary layer as well as the profile of NO along the η coordinate. We have selected the following conditions for pressure and β: p_e = 1000 N/m^2 and β = 5000 s^{-1}, while we consider different values of the T_e/T_w pairs. We present results for both choices of the rates of the process yielding NO from vibrationally excited N_2 and O atoms.

We will call the results obtained by using Eq. (23) model I, and those obtained by Eqs. (30–33) model II. Let us first examine the I results. Figures 1–3, parts a and b, report the vibrational distributions of N_2 (1a–3a) and of O_2 (1b–3b) at different η values, while Figs. 1c–3c report the profile of NO as a function of η. The figures differ from the value of the surface temperature that assumes three different values (T_w = 300, Fig.1; 500, Fig.2; and 1000 K, Fig. 3), while the other parameters (p_e = 1000 N/m^2, T_e = 5000 K; β = 5000 s^{-1}) are kept constants.

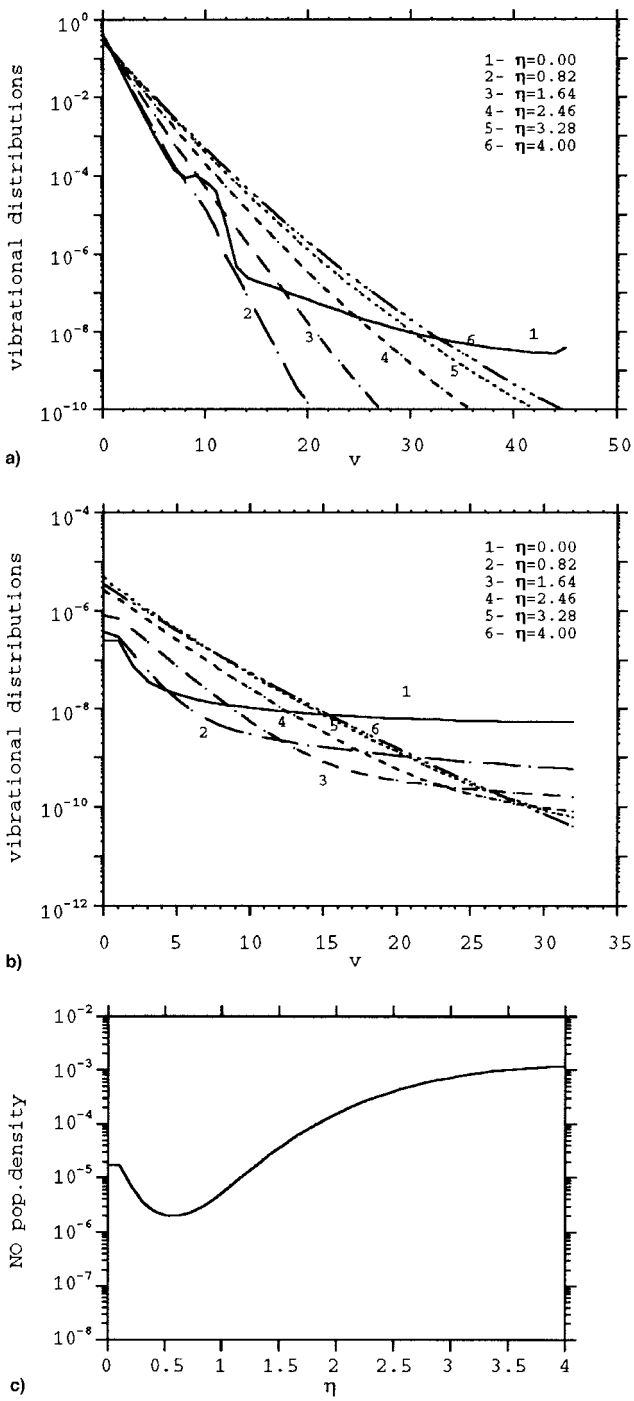

Fig. 2 Vibrational distributions of a) N_2 and b) O_2 at different η values, and c) NO profile as a function of η at T_w = 500 K, T_e = 5000 K, p_e = 1000 N/m^2, and β = 5000 s^{-1}.

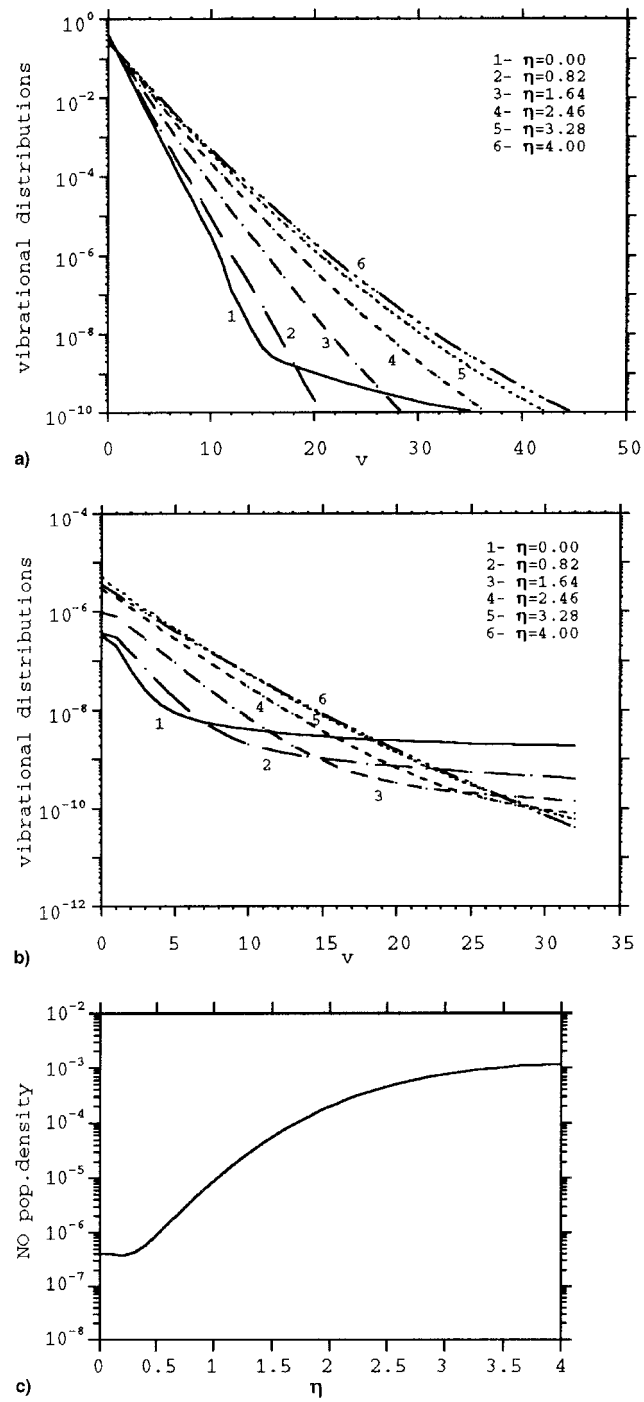

Fig. 3 Vibrational distributions of a) N_2 and b) O_2 at different η values, and c) NO profile as a function of η at T_w = 1000 K, T_e = 5000 K, p_e = 1000 N/m^2, and β = 5000 s^{-1}.

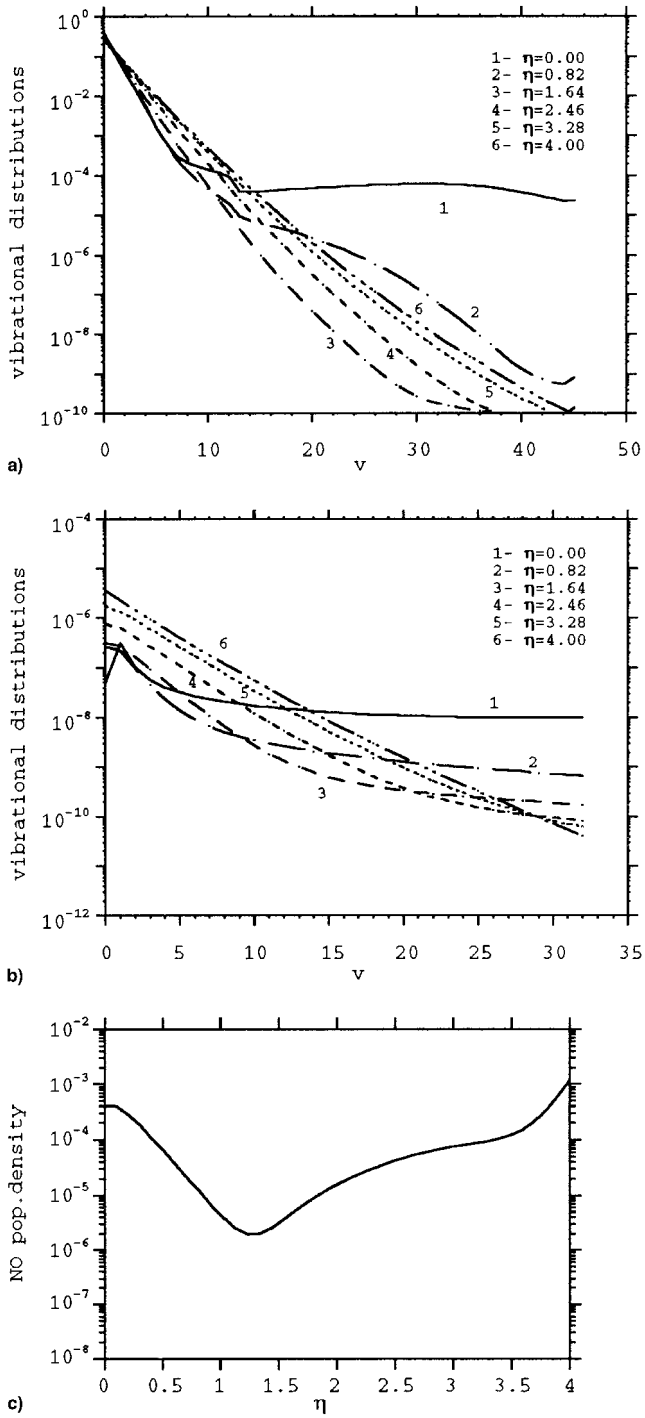

Fig. 4 Vibrational distributions of a) N_2 and b) O_2 at different η values, and c) NO profile as a function of η at T_w = 300 K, T_e = 5000 K, po_e = 1000 N/m^2, and β = 5000 s^{-1}, and using rates from Ref. 15 for process (9).

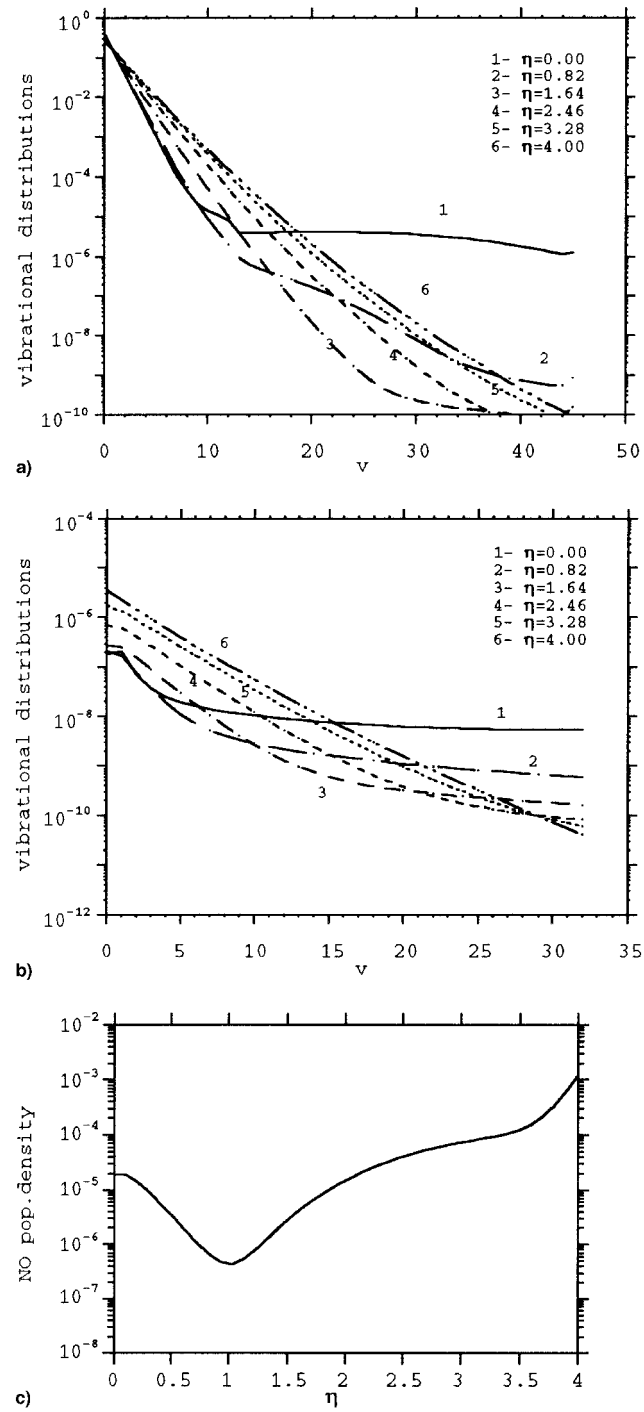

Fig. 5 Vibrational distributions of a) N_2 and b) O_2 at different η values and c) NO profile as a function of η at T_w = 500 K, T_e = 5000 K, p_e = 1000 N/m^2, and β = 5000 s^{-1}, and using rates from Ref. 15 for process (9).

Recall that the temperature profile degrades from the edge of the boundary layer (η = 4) to the surface (η = 0), so that the temperature decreases with decreasing η. Inspection of the different figures shows a highly nonequilibrium character of the vibrational distribution of N_2 near the surface. This behavior tends to disappear with increasing surface temperature. The same trend is shown by the vibrational distributions of O_2, the concentration of which is very small because of the high dissociation degree of O_2.

Both distributions are pumped by the recombination process, which populates the high-lying vibrational levels of the diatomic species. The introduced vibrational quanta are spread by V–V and V–T energy exchanges processes; in the case of N_2, the reaction for the formation of NO represents a strong deactivation channel for the corresponding vibrational distribution. The small concentration of molecular O_2 for the studied conditions justifies the neglection of V–V' energy exchange processes between vibrationally excited O_2 and N_2 molecules.

The role of surface temperature in decreasing the nonequilibrium character of the N_2 vibrational distributions is reflected also on the profile of NO concentration along η. We observe that the flat minimum present in the profile at T_w = 300 K tends to disappear at T_w = 1000 K with an intermediate be-

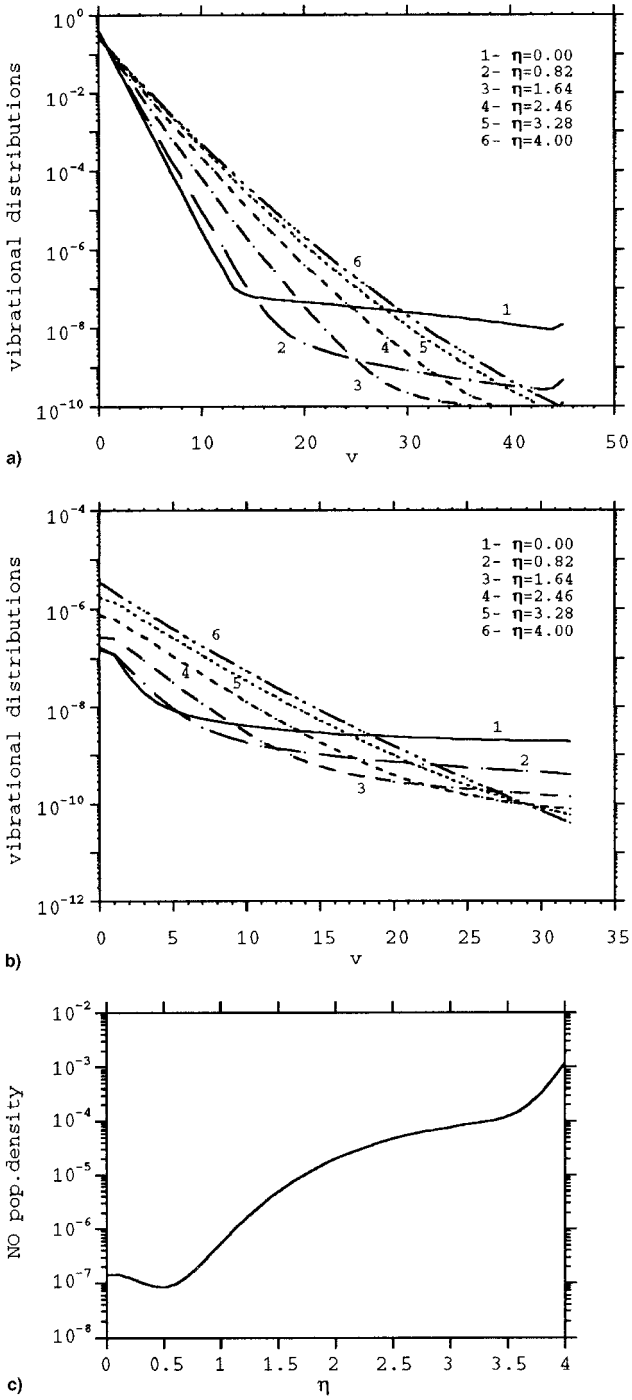

Fig. 6 Vibrational distributions of a) N_2 and b) O_2 at different η values, and c) NO profile as a function of η at T_w = 1000 K, T_e = 5000 K, p_e = 1000 N/m^2, and β = 5000 s^{-1}, and using rates from Ref. 15 for process (9).

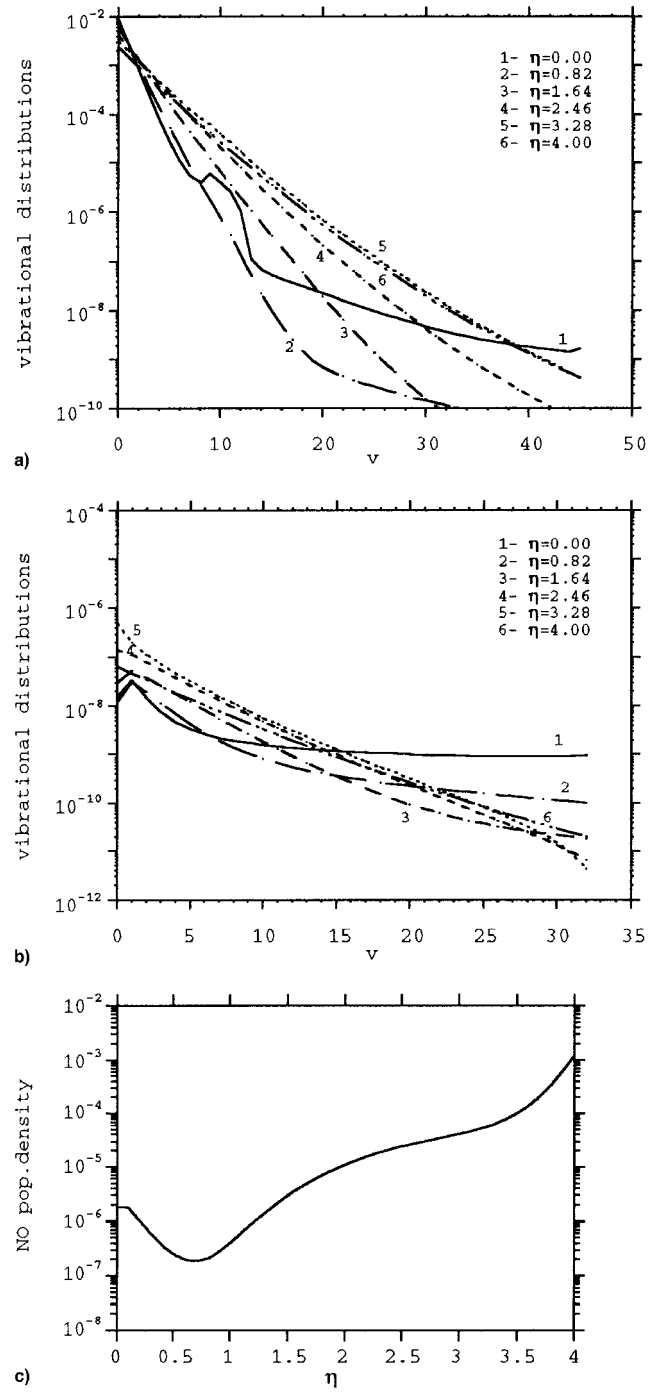

Fig. 7 Vibrational distributions of a) N_2 and b) O_2 at different η values, and c) NO profile as a function of η at T_w = 1000 K, T_e = 7000 K, p_e = 1000 N/m^2, and β = 5000 s^{-1}.

havior at T_w = 500 K. Note also that the concentration of NO decreases by orders of magnitude passing from T_w = 300–1000 K. This is because of the decrease of the reaction rate of process (9), with increasing T_w caused by the corresponding decrease of the vibrational distributions of N_2.

Figures 4–6 report similar results for model II. These results can be read on the same basis of Figures 1–3. Qualitatively, we obtain the same results. On the other hand, strong differences are observed in the absolute values of the vibrational distributions of N_2. In this case (i.e., case II), the vibrational distributions are much more pumped as compared with the I results, as a consequence of the lower reaction rates for process (9). The lower reaction rates used in model II decrease the deactivation of the vibrational distribution, thus increasing their concentration with respect to the corresponding values of model I. The large differences in the vibrational populations do not strongly modify the NO profile in models I and II because the larger vibrational distributions in model I are accompanied by lower reaction rates in the same model, so that the rate of formation of NO does not strongly change in the two models.

A similar behavior is found by increasing T_e: results for the two models have been reported in Figs. 7a–7c.

So far, all of the results have been obtained by neglecting reaction (11). To study the sensitivity of our results to the insertion of this process, we have inserted it in model I. Com-

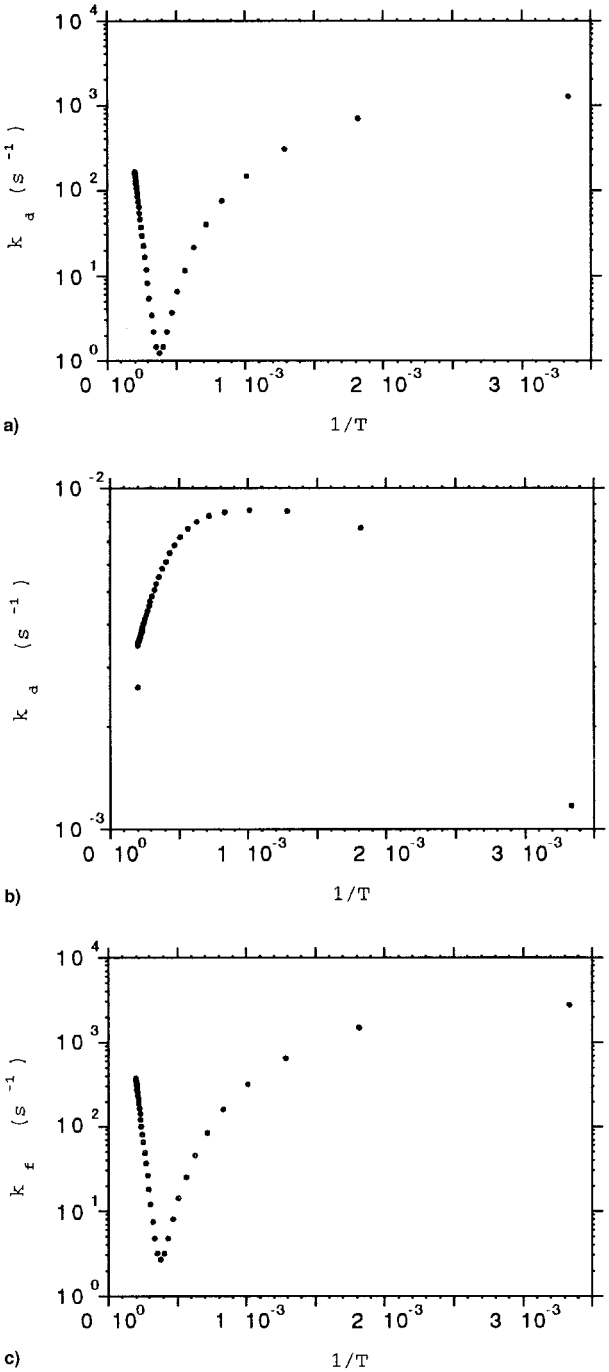

Fig. 8 Pseudo-first-order dissociation constant of a) N_2 and b) O_2, and c) NO formation rate vs $1/T$ at $T_w = 300$ K, $T_e = 5000$ K, $p_e = 1000$ N/m^2 and $\beta = 5000$ s^{-1}, and using rates from Ref. 15 for process (9).

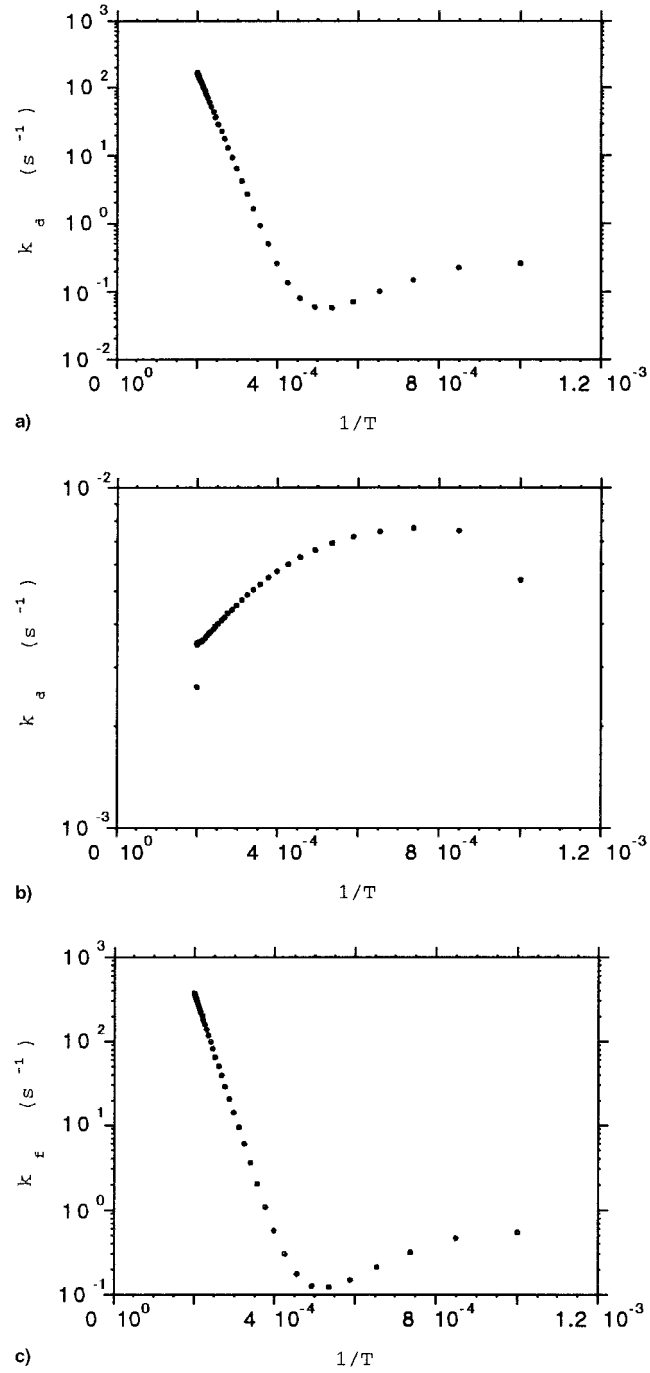

Fig. 9 Pseudo-first-order dissociation constant of a) N_2 and b) O_2, and c) NO formation rate vs $1/T$ at $T_w = 1000$ K, $T_e = 5000$ K, $p_e = 1000$ N/m^2, and $\beta = 5000$ s^{-1}, and using rates from Ref. 15 for process (9).

parison of the obtained results with those of Fig. 7 shows that only the NO profile is affected by reaction (11) from $\eta = 1$ to 0. In particular, the NO concentration calculated by inserting reaction (11) is one order of magnitude higher at $\eta = 0.7$ and three times higher at $\eta = 0$ than the corresponding values obtained without inserting reaction (11). This implies that reactions (9) and (11) are competitive in forming NO in the low and intermediate temperature ranges.

Dissociation and Reaction Rates

The large deviations of vibrational distributions from Boltzmann ones should be indicative of nonArrhenius behavior of dissociation and reaction rates along the η coordinate, i.e., along the instantaneous temperature met by the molecules in the boundary layer.

According to the ladder-climbing model, we can define a dissociation rate for N_2 (part cm^{-3} s^{-1}) as the sum of the different energy exchange processes

$$\frac{\mathrm{dN(46)}}{\mathrm{d}t} = \sum_w KN^{45,\mathrm{N}}_{w,w-1}\mathrm{N_2}(45)\mathrm{N_2}(w) + K2N_{45,\mathrm{N}}\mathrm{N_2}(45)\mathrm{N_2} + \sum_w K1N_{w,\mathrm{N}}\mathrm{N_2}(w)\mathrm{N} + \sum_v Q^{\mathrm{O,NO}}_{\mathrm{N_2}(v),\mathrm{N}}\mathrm{N_2}(v)\mathrm{O} = k_d\mathrm{N_{tot}} \qquad (38)$$

The first term on the right-hand side of Eq. (38) is the contribution from the V–V terms, the second and the third ones are

from the $V-T$ terms induced by molecules and atoms, and the last one is from process (9). N_{tot} is the total number density so that $k_d\,(s^{-1})$ is a pseudo-first-order dissociation constant. A similar equation holds for O_2.

Concerning NO formation, we define a pseudo-first-order formation rate $k_f\,(s^{-1})$ as

$$k_f = \sum_v N_2(v) Q^{O,NO}_{N_2(v),N} \tag{39}$$

The different pseudo-first-order rates have been reported in Figs. 8 and 9 for the same conditions of Figs. 4 and 6 (model II). A strong non-Arrhenius behavior of the rates vs instantaneous $1/T$ values appears, the nonequilibrium character tending to decrease with increasing T_w. In particular, the pseudo-first-order dissociation constant of N_2 presents a deep minimum vs $1/T$ at $T_w = 300$ K, i.e., the dissociation constant follows an Arrhenius behavior at high temperature, while a given temperature on the dissociation rate increases with decreasing gas temperature (increased values of $1/T$). A similar behavior is observed at $T_w = 500$ K. At $T_w = 1000$ K (Fig. 9) the nonequilibrium character of rates is strongly reduced.

A similar behavior is presented by the rate of the formation of NO (Figs. 8c and 9c), since both the dissociation of N_2 and the formation of NO are strictly linked to the nonequilibrium vibrational distribution of N_2.

Some differences are observed with the dissociation of O_2: in this case we observe a completely non-Arrhenius behavior of the dissociation constant caused by the corresponding nonequilibrium vibrational distributions. In this case, however, the dissociation rate is very small because the O_2 molecule is almost completely dissociated in the boundary layer.

The results depend on the input data: in particular the NO profile depends on the used set of vibrational state depending rates. The two sets of cross sections used in the present work can be considered as the upper (model I) and lower (model II) limits. The rates recently calculated[19–21] are in between the corresponding values calculated with the two used models.

Conclusions

In this paper we have presented results of calculations of vibrational distributions and dissociation, and the formation rate constants in the boundary layer of re-entering body in atmospheric air. The results confirm previous ones obtained for pure nitrogen, i.e., the presence of highly non-equilibrium vibrational distributions as well as the recombination process. These distributions promote the formation of NO through the reaction of vibrationally excited molecules with atomic oxygen. A corresponding non-Arrhenius behavior of the different rate constants is observed along the coordinate perpendicular to the body assumed to be noncatalytic.

The present results indicate that the magnitude of nonequilibrium increases with decreasing surface temperatures. In this sense, our results should be very close to those that can be obtained in expansion flows through a nozzle when the translational temperature suddenly decreases and the nonequilibrium vibrational kinetics finds an ideal situation for creating non-Boltzmann vibrational distribution functions. The importance of the vibrational coupling in affecting NO formation behind shock waves has been shown.[21] However, the vibrational temperature is less than the translational one, so that the nonequilibrium effects are less important than those discussed in this paper.

The present approach based on the simultaneous solution of a ladder-climbing model for molecular species should be inserted in more robust fluid dynamic codes to see how this kind of nonequilibrium can affect the whole flowfields and the temperature profiles around the body. In doing so one should attempt to insert in the kinetics the presence of the vibrational levels of NO as well as the presence of electronically excited states of N_2, O_2, and NO that have been completely disregarded in this present paper.

Acknowledgments

This work has been partially supported by Agenzia Spaziale Italiana and Ministero Universita Ricerca Scientifica e Tecnologica. The authors thank Colonna for useful discussions.

References

[1]Armenise, I., Capitelli, M., and Gorse, C., "On the Coupling of Non-Equilibrium Vibrational Kinetics and Dissociation-Recombination Processes in the Boundary Layer Surrounding a Hypersonic Re-Entry Vehicle," European Space Agency, SP-367, 1995, pp. 287–292.

[2]Armenise, I., Capitelli, M., and Gorse, C., "Fundamental Aspects of the Coupling of Non-Equilibrium Vibrational Kinetics and Dissociation-Recombination Processes with the Boundary Layer Fluid Dynamics in N_2 and Air Hypersonic Flows," *NATO ASI Molecular Physics and Hypersonic Flows*, Kluwer, Dordrecht, The Netherlands, 1996, pp. 703–716.

[3]Armenise, I., Capitelli, M., and Gorse, C., "Non Equilibrium Vibrational Distributions and Non Arrhenius Dissociation Constants of N_2 in Hypersonic Layer," *J. Thermophysics and Heat Transfer* (to be published).

[4]Capitelli, M., and Molinari, E., "Kinetics of Dissociation Processes in Plasmas in the Low and Intermediate Pressure Range," *Topics in Current Chemistry*, Vol. 90, 1980, pp. 59–109.

[5]Armenise, I., Capitelli, M., Celiberto, R., Colonna, G., Gorse, C., and Laganà, A., "The Effect of N + N_2 Collisions on the Non-Equilibrium Vibrational Distributions of Nitrogen Under Re-Entry Conditions," *Chemical Physics Letters*, Vol. 227, Nos. 1, 2, 1994, pp. 157–163.

[6]Armenise, I., Capitelli, M., Colonna, G., and Gorse, C., "Non-equilibrium Vibrational Kinetics in the Boundary Layer of Re-Entering Bodies," *Journal of Thermophysics and Heat Transfer*, Vol. 10, No. 3, 1996, pp. 397–405.

[7]Billing, G. D., and Fisher, E. R., "VV and VT Rate Coefficients in N2 by a Quantum-Classical Model," *Chemical Physics*, Vol. 43, No. 1, 1979, pp. 395–401.

[8]Laganà, A., and Garcia, E., "Temperature Dependence of N + N_2 Rate Coefficients," *Journal of Physical Chemistry*, Vol. 98, No. 2, 1994, pp. 502–507.

[9]Armenise, I., Capitelli, M., Garcia, E., Gorse, C., Laganà, A., and Longo, S., "Deactivation Dynamics of Vibrationally Excited Nitrogen Molecules by Nitrogen Atoms: Effects on Non-Equilibrium Vibrational Distribution and Dissociation Rates of Nitrogen Under Electrical Discharges," *Chemical Physics Letters*, Vol. 200, No. 3, 1992, pp. 597–604.

[10]Billing, G. D., and Kolesnick, R. E., "Vibrational Relaxation of Oxygen. State to State Rate Constants," *Chemical Physics Letters*, Vol. 200, No. 4, 1992, pp. 382–386.

[11]Cacciatore, M., Capitelli, M., and Dilonardo, M., "Non-Equilibrium Vibrational Population and Dissociation Rates of Oxygen in Electrical Discharges: The Role of Atoms and of the Recombination Process," *Beiträge aus der Plasma Physik*, Vol. 18, No. 5, 1978, pp. 279–299.

[12]Billing, G. D., "VV and VT Rates in N_2-O_2 Collisions," *Chemical Physics*, Vol. 179, No. 3, 1994, pp. 463–467.

[13]Mnatsakanyan, A. K., and Naidis, G. V., "The Vibrational-Energy Balance in a Discharge in Air," *High Temperature*, Vol. 4, No. 3, 1985, pp. 506–513.

[14]Gordiets, B. F., *Vibrational Kinetics of Molecules and Infrared Emission in the Terrestrial Ionosphere*, Preprint 117, Physical Inst. of Academy of Science, Moscow, 1990.

[15]Park, C., "A Review of Reaction Rates in High Temperature Air," AIAA Paper 89-1740, June 1989.

[16]Gordiets, B. F., Ferreira, C. M., Guerra, V. L., Loureiro, J. M. A. H., Nahorny, J., Pagnon, D., Touzeau, M., and Vialle, M., "Kinetic Model of a Low-Pressure N_2-O_2 Flowing Glow Discharge," *IEEE Transactions on Plasma Science*, Vol. 23, No. 4, 1995, pp. 750–767.

[17]Doroshenko, V. M., Kudryavtsev, N. N., Novikov, S. S., and Smetanin, V. V., "Influence of the Formation of Vibrationally Excited Molecules in Gas Phase Recombination on the Surface Heat Flux," *High Temperature*, Vol. 28, No. 1, 1990, pp. 82–89.

[18]Armenise, I., Capitelli, M., Colonna, G., Koudriavtsev, N., and

Smetanin, V., "Nonequilibrium Vibrational Kinetics During Hypersonic Flow of a Solid Body in Nitrogen and Its Influence on the Surface Heat Flux," *Plasma Chemistry and Plasma Processing*, Vol. 15, No. 3, 1995, pp. 501–528.

[19]Candler, G. V., Bose, D., and Olejniczak, J., "Interfacing Nonequilibrium Models with Computational Fluid Dynamics Methods," *NATO ASI Molecular Physics and Hypersonic Flows*, Kluwer, Dordrecht, The Netherlands, 1996, pp. 625–644.

[20]Bose, D., and Candler, G. V., "Thermal Rate Constants of the $N_2 + O \rightarrow NO + N$ Reaction Using *Ab Initio* 3A" and 3A' Potential Energy Surfaces," *Journal of Chemical Physics*, Vol. 104, No. 8, 1996, pp. 2825–2833.

[21]Treanor, C. E., Adamovich, I. V., Williams, M. J., and Rich, J. W., "Kinetics of Nitric Oxide Formation Behind Shock Waves," *Journal of Thermophysics and Heat Transfer*, Vol. 10, No. 2, 1996, pp. 193–199.